PCCP

Branching ratios for competing channels in the reaction of HOCO radicals with NO

Rouslan V. Olkhov, Qiang Li, Michael C. Osborne and Ian W. M. Smith*

School of Chemistry, The University of Birmingham, Edgbaston, Birmingham, UK B15 2TT.
E-mail: i.w.m.smith@bham.ac.uk; Fax: +44 121 414 4426

Received 9th July 2001, Accepted 16th August 2001
First published as an Advance Article on the web 24th September 2001

The yields of CO_2 from the reactions of HOCO radicals with O_2 and with NO have been compared using the technique of time-resolved infrared absorption. In two separate series of experiments, HOCO radicals have been generated by (i) broadband ultraviolet photolysis of acrylic acid ($CH_2CHCOOH$) and (ii) the reaction, $Cl + HCOOH \rightarrow HCl + HOCO$, following pulsed laser photolysis of Cl_2 at 351 nm. In the latter experiments, the observed CO_2 yields were corrected for the loss of Cl atoms by the reactions $Cl + NO + He \rightarrow ClNO + He$ and $Cl + ClNO \rightarrow Cl_2 + NO$. Our measurements on the rate of $Cl + NO + He$ yield a value of the third-order rate constant of $(5.1 \pm 0.7) \times 10^{-32}$ cm^6 $molecule^{-2}$ s^{-1}. The results of the main experiments show that the yield of CO_2 from the reaction between NO + HOCO is appreciably less than that from O_2 + HOCO and is dependent on the total pressure in the range 10 to 100 Torr. We interpret this as showing that the reactions $HOCO + NO \rightarrow HNO + CO_2$ and $HOCO + NO(+M) \rightarrow HOC(O)NO(+M)$ occur at similar rates, with the latter reaction being favoured at the higher total pressure.

Introduction

The hydroxy formyl radical HOCO is of great interest as a transitory intermediate in the reaction between OH radicals and CO. This reaction is very important since, in the combustion of hydrocarbons and their oxidation in the Earth's atmosphere, it is virtually the only mechanism for converting CO to CO_2, the final oxidation product of fuel-based carbon. At ground level in the atmosphere, the initial reaction between OH and CO occurs, at competitive rates,[1,2] by two parallel channels, both involving energised HOCO radicals as an intermediate:

$$OH + CO \leftrightarrows (HOCO)^{\dagger} \longrightarrow H + CO_2 \quad (1a, -1a)$$

$$\xrightarrow{+M} HOCO \quad (1b)$$

In practice, in an atmosphere of which 20% is O_2, reactions (1a) and (1b) lead to the same result, since the radical product of each is rapidly converted to HO_2 by one or other of the two reactions:[1,2]

$$H + O_2 + M \rightarrow HO_2 + M \quad (2)$$

or

$$HOCO + O_2 \rightarrow HO_2 + CO_2, \quad \Delta_r H^0 = -156 \text{ kJ mol}^{-1} \quad (3)$$

The facts that OH and CO react by channels (1a) and (1b), that both reactions proceed *via* an energised HOCO intermediate, and that this intermediate re-dissociates to OH + CO at a rate comparable with those of dissociation to H + CO_2 and of collisional stabilisation account for the unusual temperature and pressure dependence of this reaction.[1–6] Moreover, the presence of an attractive potential well on the reaction path, corresponding to the 154 kJ mol^{-1} binding energy of OH to CO,[7] gives rise to unusual reaction dynamics. These have been explored for the forward reaction (1a) in the gas-phase,[8–10] and for the reverse reaction (−1a) between H atoms and CO_2, both in gas-phase studies using translationally 'hot' H atoms[11,12] and in weakly bound dimers of CO_2 bound to HX (X = Br, I).[13,14]

Despite the wide interest in its role as a reaction intermediate, there have been relatively few studies of the reactions of HOCO itself. Following its early spectroscopic detection in low temperature matrices,[15,16] some features of the infrared spectrum of gas-phase HOCO have been characterised,[17,18] using the photolysis of a carboxylic acid (RCOOH) to generate the radical. There have been three determinations of the room temperature rate constant for reaction (3),[19–21] all at total pressures below 10 Torr. The conditions and results of these studies are summarised in Table 1. The three measurements are consistent with one another, and it is generally assumed that reaction proceeds exclusively *via* the channel yielding HO_2 and CO_2. However, as far as we are aware, there is no evidence as to whether this reaction proceeds by direct H-atom abstraction or by initial addition of O_2 to the C-atom to generate a peroxy radical intermediate which then

Table 1 Previous kinetic studies of the reactions of HOCO radicals with O_2 and with NO at 298 K

Method of generating HOCO	Method of detecting HOCO	$k_3/10^{-12}$ cm^3 $molecule^{-1}$ s^{-1}	$k_4/10^{-12}$ cm^3 $molecule^{-1}$ s^{-1}	Ref.
Pulsed laser photolysis of *trans*-C_2H_3COOH	IR absorption using cw difference-frequency laser	1.9 ± 0.2	$2.4_5 \pm 0.2$	19
Cl + HCOOH in flow system	Laser magnetic resonance	$1.6_4 \pm 0.25$		20
Cl + HCOOH in flow system	Photoionisation mass spectrometry	$1.4_4 \pm 0.3$		21

DOI: 10.1039/b106071f

decomposes to $HO_2 + CO_2$ following internal H-atom transfer.

There has apparently been only one study of the reaction of HOCO with NO, which like O_2 is a radical but has one rather than two unpaired electrons. Observing time-resolved absorption of a continuous, frequency difference, infrared laser to monitor kinetic decays of the HOCO concentrations, Petty *et al.*[19] measured a rate constant slightly higher than that for HOCO + O_2 (see Table 1). With NO, there are alternative bimolecular channels:

$$HOCO + NO \rightarrow HNO + CO_2, \quad \Delta_r H^0 = -161 \text{ kJ mol}^{-1} \qquad (4a)$$

and

$$HOCO + NO \rightarrow HONO + CO, \quad \Delta_r H^0 = -57 \text{ kJ mol}^{-1} \qquad (4b)$$

Petty *et al.* were able to detect absorptions assigned to HNO and HONO but were unable to determine the branching ratio for channels (4a) and (4b), in part because the absorption cross-sections for transitions of the observed species are not known.

We have carried out a number of experiments related to the formation of HOCO and of its reactions using time-resolved absorption of monochromatic, narrowband, radiation from tunable diode lasers to observe the production of CO_2 and CO in these systems and hence to measure the yields and progress of the reactions. In an earlier paper,[22] we reported the results of studies on the broadband ultraviolet photodissociation of two carboxylic acids (RCOOH), trifluoroacetic acid (R = CF_3) and acrylic acid (R = CH_2CH). It was shown that both these photolyses occur by at least three competing channels: to HOCO + R; to CO_2 (+R + H or +RH); and to CO (+R + OH or +ROH).

The present paper describes experiments on the reactions of HOCO with O_2 and of HOCO with NO that were designed to determine the relative yields of CO_2 in these two reactions. In initial, preliminary, experiments, HOCO radicals were generated either by broadband ultraviolet photolysis of C_2H_3COOH[22] or by the reaction:[20,21,23,24]

$$Cl + HCOOH \rightarrow HCl + HOCO, \quad \Delta_r H^0 = -58 \text{ kJ mol}^{-1} \qquad (5)$$

where Cl atoms were generated by photodissociation of Cl_2 using broadband radiation limited to wavelengths above *ca.* 300 nm. To our surprise, these experiments indicated that the CO_2 yield was lower from NO + HOCO than from O_2 + HOCO and that the ratio of yields depended on the total pressure. Moreover, we were unable to detect CO, the coproduct with HONO of reaction (4b), suggesting that channel (4b) makes, at most, a minor contribution to the overall rate of reaction between HOCO and NO.

As reaction (5) is only moderately exothermic, it is expected to produce HOCO radicals without significant internal excitation,[20,21] and so this source of HOCO has been used in subsequent experiments designed to explore the CO_2 yields from these reactions in more depth. In this paper, we emphasise the results of these later experiments, in which the broadband flashlamp was replaced by an excimer laser. It was operated on XeF and therefore provided monochromatic photolysis light at 351 nm.

In fact, in experiments utilising reaction (5) as the source of HOCO radicals, there are two causes for the reduction in the CO_2 yield. First, the yield of HOCO from reaction (5) ($^{Cl}Y_{HOCO}$) may be reduced by the successive reactions:

$$Cl + NO + He \rightarrow ClNO + He \qquad (6)$$

$$Cl + ClNO \rightarrow Cl_2 + NO \qquad (7)$$

competing with reaction (5) for the available Cl atoms. Second, the yield of CO_2 from the reaction of NO with HOCO ($^{HOCO}Y_{CO_2}$) could be reduced by the existence of a third, pressure-dependent, channel in this reaction, presumably:

$$HOCO + NO + M \rightarrow HOC(O)NO + M \qquad (4c)$$

In order to make the necessary corrections for the effect of reactions (6) and (7) and hence find $^{HOCO}Y_{CO_2}$, the rate of reaction (6) was also measured under our experimental conditions by following the rate of formation of ClNO by time-resolved infrared absorption. Having made these corrections, the lower yield of CO_2 from NO + HOCO compared with O_2 + HOCO has been confirmed, as has the pressure-dependence of this effect, indicating the importance of reaction (4c).

Experimental

The present experiments all depend on time-resolved measurements of the absorption of radiation from tunable diode lasers. Two modifications of the apparatus have been used. The first, used in the preliminary experiments and referred to as Experiment A, is similar to that used previously[22,23] and will only be described briefly here. The second apparatus (Experiment B) was used for most of the measurements whose results are presented here.

Experiment A

As stated in the Introduction, HOCO radicals were prepared in two ways, by photolysis of acrylic acid, $CH_2CHCOOH$, and by reaction (5). The photolysis light source was provided by an annular flash lamp positioned around a cylindrical reaction cell. In experiments utilising acrylic acid, the reaction vessel was constructed from quartz. It was replaced by a Pyrex vessel when HOCO was generated from formic acid *via* reaction (5), so that only light of wavelengths >300 nm entered the reaction vessel and only Cl_2, not HCOOH, was photolysed. The infrared radiation was provided by a liquid nitrogen cooled diode laser system (Mutek GmbH, MDS 1150). The methods of determining and tuning the frequency of the diode output have been described previously.[22] Collimating optics were employed to generate a suitable probe beam which then made a single pass along the length (*ca.* 80 cm) of the reaction cell. A single mode of the infrared probe beam was selected by a monochromator and then monitored by a liquid N_2 cooled InSb photovoltaic detector. An AC coupled amplifier was used in conjunction with the detector and its output was passed to a digital oscilloscope for storage. Generally *ca.* 20 traces were averaged before subsequent processing. The time response of the detector–amplifier combination was about 10 μs.

Experiment B

In these experiments, we employed a pulsed excimer laser as the photolysis source and a multi-pass arrangement for the infrared probe laser. A schematic diagram of the apparatus is shown in Fig. 1. The tubular Pyrex reaction vessel, which was *ca.* 1 m long and 80 mm diameter, was fitted with Herriott cell mirrors arranged so that the probe beam made 16 passes through the cell. The output at 351 nm from a XeF excimer laser (Lambda Physik, Compex 102 excimer laser) entered the reaction vessel through one of the mirrors, which has a central hole, and irradiated a cylindrical volume around the longitudinal axis with 20–60 mJ $(pulse)^{-1}$ of laser light. At 351 nm, only Cl_2 has significant absorption, leading to its dissociation and eventually to the production of HOCO and/or ClNO in reactions (5) and (6). The excimer laser was fired at only 0.1–

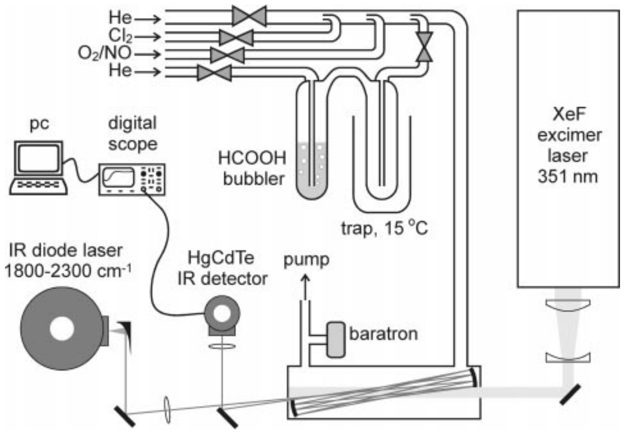

Fig. 1 Apparatus used to study (a) the kinetics of the reaction between Cl atoms and NO, and (b) the yields of CO_2 from the reaction of HOCO radicals with O_2 and NO; the HOCO radicals being produced from the Cl + HCOOH reaction.

0.2 Hz so that the gas mixture in the cell could be refreshed between successive photolysis laser shots. The total path length over which the ultraviolet photolysis and infrared probe beams overlapped was estimated as *ca.* 8 m. The intensity of the emerging infrared beam was measured by a fast (20 MHz) HgCdTe infrared detector coupled to a DC amplifier, then collected in the desired time window by the digital oscilloscope, and ultimately transferred to a PC for further analysis.

Variations in the concentration of one of the final products were monitored by time-resolved infrared absorption at an appropriate frequency. For CO_2 formed in reactions (3) and (4a), measurements were made at 2334.16 cm^{1}, *i.e.* on the P(18) line in the ν_3 band. However, under our experimental conditions, lines in the ν_1 fundamental band of ClNO were strongly overlapped and, to our knowledge, the rotational structure of this band is still unassigned. Consequently, we made observations at the peak of the R branch absorption in this band at *ca.* 1830 cm^{-1}. The tunable infrared laser source was the same as before. A single 90° off-axis parabolic mirror was used as a collimating element for the highly divergent diode laser radiation.

In all the experiments, it was essential to enclose and purge the complete path of the infrared probe beam with nitrogen to eliminate background absorptions by CO_2 in the atmosphere. The main advantage of using a pulsed laser for photolysis (Experiment B) rather than a flashlamp (Experiment A) was the better time resolution that could be achieved. In addition, the single laser wavelength of 351 nm ensured that only Cl_2 was photolysed.

In both sets of experiments, a Pyrex vacuum system consisting of several flow lines fitted with 20 l storage bulbs, greaseless stopcocks and electronic mass flow controllers was used to handle gases. One of the lines included a bubbler in order to introduce a controlled flow of the vapour of a liquid reagent. The flows from different lines were mixed immediately before entering the reaction vessel. The gas mixture containing desired amounts of HCOOH, Cl_2 and O_2/NO in an excess of He was continuously flowed through the reaction vessel. Formic acid (>98%) or acrylic acid (99.5%) was delivered *via* the bubbler in a flow of He, Cl_2 (UHP grade) was premixed with He in the ratio 1 : 5 and delivered from a storage bulb, O_2 (99.6%), NO (99.5%) and He (GC grade) were taken directly from cylinders without further purification.

Results

In our first experiments (of type A), HOCO radicals were generated by broadband ultraviolet photolysis of $CH_2CHCOOH$, and the relative yields of CO_2 from three separate but related experiments were determined from the absorbance measured at long time delays (>5 ms). In each experiment in a set, the concentrations of the $CH_2CHCOOH$ and the He diluent were kept constant, and traces of absorbance were recorded: (a) from a mixture containing O_2, (b) from a mixture containing NO and (c) in the absence of both these gases. This procedure was necessary because CO_2 is formed directly in the photolysis of $CH_2CHCOOH$ under these conditions. Consequently, the yields of CO_2 from reactions (3) and (4a) are reflected in differences in the absorbances at long time between (a) and (c) and between (b) and (c). Fig. 2 shows an example of typical results from such experiments. Comparisons of traces (a) and (b) demonstrate clearly that there is a lower yield of CO_2 from NO + HOCO than from O_2 + HOCO.

Two series of experiments of this kind were performed at partial pressures of NO and O_2 of between 500 and 600 mTorr. With the total pressure at 10 Torr, the partial pressure of $CH_2CHCOOH$ was varied between 8 and 40 mTorr. With the total pressure at 50 Torr, the partial pressure of $CH_2CHCOOH$ was varied between 3 and 30 mTorr. In both cases, the additional yields of CO_2 from experiments with NO and O_2 present were found to be independent of [$CH_2CHCOOH$]. At 10 Torr, the ratio of yields was found to be (0.51 ± 0.04) and at 50 Torr it was determined to be (0.30 ± 0.06). In both cases, the cited errors correspond to $\pm 2\sigma$, including only the statistical error in the data.

Petty *et al.*[19] have reported the detection of the HONO product of reaction (4b) between NO and HOCO. With the laser diodes that we have available it was impossible to look for HONO but we searched for CO, the co-product of reaction (4b), like Petty *et al.* using photolysis of acrylic acid as the source of HOCO. CO is one of the products of the ultraviolet photolysis of $CH_2CHCOOH$ under the conditions of our experiments, being formed in comparable amounts to HOCO.[22] In the present experiments, despite a number of attempts, we were unable to detect any significant increase in the CO yield when NO was added. Estimating that we should have been able to observe a 5% increase in the CO absorbance over that from photolysis alone, we estimate that the branching ratio to HONO + CO in the reaction between HONO + NO is less than 0.05.

Preliminary experiments, using reaction (5) as a source of HOCO, were carried out in experiments of type A. However, the effect on the results of the association reaction between Cl atoms and NO was not fully appreciated at that time, and consequently less than ideal conditions were chosen for these measurements. Here, we only report the results from the extensive measurements that we have made in the experiments of type B.

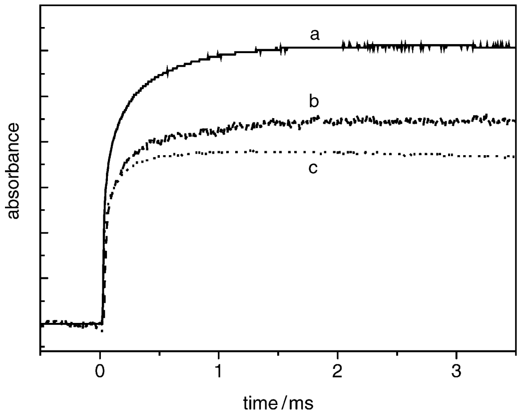

Fig. 2 Comparison of CO_2 product yields from photolysis of mixtures of 29.6 mTorr C_2H_3COOH in He at a total pressure of 50 Torr, (a) with 760 mTorr O_2, (b) with 630 mTorr NO and (c) with neither O_2 nor NO added.

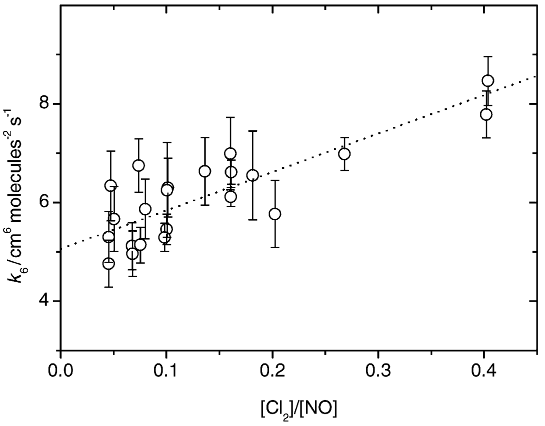

Fig. 3 Rate constants for the association of Cl atoms with NO shown at different [Cl$_2$]/[NO] ratios. Evaluation of the Cl + NO rate constant with k_7 fixed at the recommended value. Linear dependence of derived k_6 on the [Cl$_2$]/[NO] suggests that k_7 is slightly overestimated.

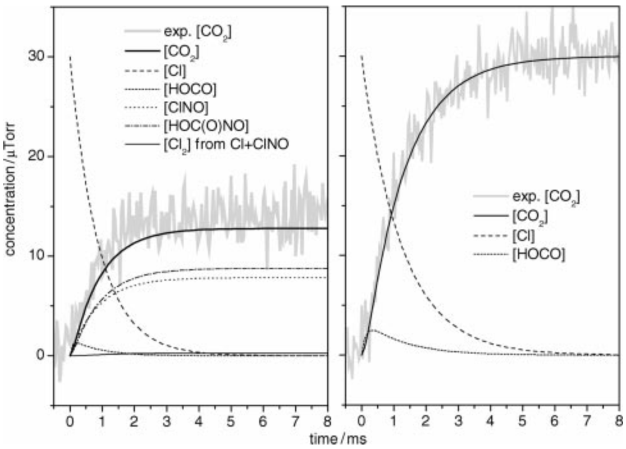

Fig. 4 Comparison of traces of infrared absorbance on the P(18) line of the (00^01,00^00) band of CO_2 from: (a) the photolysis of 10 mTorr of Cl_2 in the presence of *ca.* 350 mTorr of HCOOH and 120 mTorr NO in He at a total pressure of 50 Torr, and (b) from a similar mixture in which the NO was replaced by a similar partial pressure of O_2. The lines show the fits calculated according to the model outlined in the text.

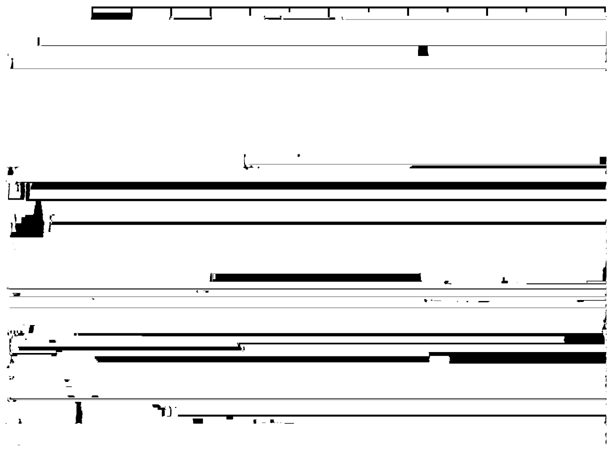

Fig. 5 Yields of CO_2 from HOCO + NO relative to those from HOCO + O_2 at different partial pressures of NO and different total pressures. The filled symbols are from experiments of type A in which HOCO radicals were generated by photolysis of $CH_2CHCOOH$ at 10 Torr (◆) and 50 Torr (■) total pressure. The open symbols are from experiments of type B in which HOCO radicals were generated from the reaction of Cl atoms with HCOOH. Experiments of this kind were carried out at 25 Torr (○), 50 Torr (□) and 100 Torr (△). Error bars shown correspond to $\pm 2\sigma$.

We begin by reporting on the experiments designed to determine the rate constant for reaction (6), which was measured so that the effect of this reaction on the measurements of total CO_2 yields could be accurately assessed. Although the rate of this reaction has been measured previously,[2,25] most of the measurements have been made with N_2 as the third-body gas. Whilst reaction (6) was likely to compete with reaction (5), and hence affect the yield of CO_2 in experiments on the reaction between NO and HOCO, the loss of Cl due to reaction (7) was estimated to be of only minor significance due to the low concentrations of both Cl atoms and ClNO. Therefore the recommended value of the rate constant for reaction (7) of 8.1×10^{-11} cm^3 molecule^{-1} s^{-1} was used in modelling calculations.

The third-order rate constant (k_6) for reaction (6) was determined by observing the time-dependence of the absorbance of ClNO following laser photolysis of Cl_2 in mixtures containing Cl_2 and NO diluted in He at total pressures between 50 and 100 Torr. The concentration of NO and the total pressure were varied in different experiments. k_6 was extracted from the traces by modelling the variation of absorbance with time, allowing k_6 to vary, with k_7 fixed at the value 8.1×10^{-11} cm^3 molecule^{-1} s^{-1} and assuming that reaction (6) was in its low pressure regime where its rate would be directly proportional to [He].

Fig. 3 shows the derived values of k_6 at different values of the ratio [Cl$_2$]/[NO]. The smaller this ratio, the less our result would be expected to depend on the assumed value of k_7. A linear extrapolation of these data to [Cl$_2$]/[NO] = 0 yields $k_6 = (5.1 \pm 0.7) \times 10^{-32}$ cm^6 molecule^{-2} s^{-1} as our best estimate of the third-order rate constant for the association of a Cl atom with NO in the presence of He as the third-body gas. This value was used in the analyses of subsequent experiments on the reaction between NO and HOCO radicals.

The yields of CO_2 from the reactions of O_2 and NO with HOCO were measured at three different total pressures, 25, 50 and 100 Torr, and for various concentrations of O_2 and NO. The yields from mixtures containing the same concentrations of O_2 and NO were compared in back-to-back experiments.

Table 2 Experiment B: Relative yields of CO_2 from reaction (4) in Cl_2/HCOOH/NO system normalised for relevant Cl_2/HCOOH/O_2 measurements and corrected for the loss of Cl atoms in reactions (6) and (7)

Total pressure/Torr	[NO]/mTorr	$^{total}Y_{CO_2}$	$^{Cl}Y_{HOCO}$	$^{HOCO}Y_{CO_2}$
25	71	0.781	0.887	0.88 ± 0.14
	114	0.762	0.833	0.91 ± 0.10
	230	0.591	0.710	0.83 ± 0.09
50	70	0.491	0.803	0.61 ± 0.08
	116	0.427	0.720	0.59 ± 0.06
	227	0.295	0.557	0.53 ± 0.08
100	73	0.299	0.687	0.44 ± 0.13
	120	0.241	0.563	0.43 ± 0.11
	240	0.153	0.393	0.39 ± 0.13

As in the experiments of type A, relative total yields of CO_2 were determined from a comparison of the absorbances at long times in the experiments with NO and O_2 present. The traces of infrared absorbances *vs.* time for one such pair of experiments are shown in Fig. 4.

It is assumed in what follows that the yield of CO_2 from the reaction of O_2 with HOCO is unity; that is, each HOCO radical is converted to one molecule of CO_2. Consequently, the relative yields from a pair of similar experiments with NO and O_2 correspond to the absolute yield of CO_2 from reaction (4) between NO and HOCO. This assumption is supported by: (a) the fact that the yields of CO_2 from experiments at different total pressures was constant, allowance having been made for the effects of pressure-broadening on the measured absorbances, and (b) the lack of any bimolecular set of products from O_2 + HOCO other than $HO_2 + CO_2$ that is thermodynamically accessible.

As in the measurements of type A, the yields of CO_2 were significantly smaller in experiments of type B when NO was present rather than O_2. In these latter experiments, it was possible, and necessary, to correct for the effects of reactions (6) and (7) in lowering the yield of HOCO from reaction (5), in order to extract the yield of CO_2 from the reaction between NO and HOCO. In fact, the total, measured, yield of CO_2, ${}^{\text{total}}Y_{CO_2}$, can be expressed as the product of ${}^{Cl}Y_{HOCO}$, the yield of HOCO from Cl atoms produced by the photolysis of Cl_2 given the competition of reaction (5) with reactions (6) and (7) and ${}^{HOCO}Y_{CO_2}$, the yield of CO_2 in the reaction between NO and HOCO; *i.e.*

$$ {}^{\text{total}}Y_{CO_2} = {}^{Cl}Y_{HOCO} \times {}^{HOCO}Y_{CO_2} $$

The value of ${}^{Cl}Y_{HOCO}$ could be calculated for each experiment on a given mixture of Cl_2, NO and He from the pseudo-first-order rate constants k_5[HCOOH] and k_6[NO][He] with an allowance made for the minor reaction (7). In order to avoid any potential uncertainty in the concentration of formic acid, due to the method of delivery *via* a bubbler and its dimerisation, the values of k_5[HCOOH] that were used were those derived from the equivalent experiments on mixtures of Cl_2, O_2 and He. Table 2 and Fig. 5 present the values of ${}^{HOCO}Y_{CO_2}$ derived from experiments of type B. They are clearly: (a) in fair agreement with the less extensive results derived from experiments of type A using acrylic acid as a source of HOCO radicals, (b) less than unity for all conditions and (c) dependent on total pressure, as expected if reaction (4c) is responsible for the reduced CO_2 in the case of reaction between NO and HOCO radicals.

Discussion

The results that we report clearly demonstrate that the yield of CO_2 from the reaction between NO and HOCO radicals is less than unity and depends on total pressure. This finding can only be rationalised by the occurrence of reaction (4c) in competition with (4a) and, to a minor extent, reaction (4b). The pressure-dependent reaction (4c) presumably arises *via* an energised collision complex which is collisionally stabilised to produce the molecule HOC(O)NO. Our measurements provide no direct evidence as to whether reaction (4a) which yields HNO + CO_2 proceeds *via* the same collision complex or *via* a direct abstraction mechanism. However, indirect evidence favours the former mechanism.

If indeed both reactions proceed *via* the same energised complex, {HOC(O)NO}*, then the mechanism becomes:

$$\begin{tikzcd} \text{NO + HOCO} \arrow[r, shift left, "k_d"] & \text{\{HOC(O)NO\}*} \arrow[l, shift left, "k_a"] \arrow[r, "k_p"] \arrow[d, "k_{He}[He]"] & \text{HNO} + CO_2 \\ & \text{HOC(O)NO} & \end{tikzcd}$$

which is similar to the mechanism that is generally accepted to operate in the reaction between OH radicals and CO.[6] In presenting this scheme, we neglect the possibility of reaction (4b) to HONO + CO, but its inclusion would not affect the simplified mathematical analysis that follows.

If a simple Lindemann analysis is performed on the above mechanism, the yield of CO_2 from reaction (4) is given by

$$ {}^{HOCO}Y_{CO_2} = \frac{k_p}{k_p + k_{He}[\text{He}]} \qquad \text{(i)} $$

so that

$$ \frac{1}{{}^{HOCO}Y_{CO_2}} = 1 + \frac{k_{He}}{k_p}[\text{He}] \qquad \text{(ii)} $$

A plot of the reciprocal of ${}^{HOCO}Y_{CO_2}$ *vs.* the pressure of He is shown in Fig. 6. The slope yields the ratio of rate constants: $k_{He}/k_p = 0.014$ Torr^{-1} or 4.2×10^{-19} cm^3 molecule^{-1}. In the spirit of unimolecular reaction rate theory, k_{He}, the rate constant for collisional deactivation of energised HOC(O)NO, can be written as the product of the rate constant ($Z°$) for all collisions between He and {HOC(O)NO}* and a factor (generally called β) allowing for departure from the strong collision limit. For He, β is often found[25] to be *ca.* 0.1 so that we can estimate k_{He} to be roughly $0.1Z° \approx 2 \times 10^6$ Torr^{-1} s^{-1} or 6.1×10^{-11} cm^3 molecule^{-1} s^{-1}. If this, admittedly crude, estimate of k_{He} is combined with the value derived for k_{He}/k_p, one obtains $k_p \approx 1.5 \times 10^8$ s^{-1} for the first-order rate constant for rearrangement and dissociation of {HOC(O)NO}* to HNO + CO_2.

Our data on the CO_2 yields provide no information about whether the {HOC(O)NO}* complexes, which are a necessary precursor to the formation of stable HOC(O)NO molecules and a likely precursor to the products HNO + CO_2, undergo redissociation to NO + HOCO at a rate competitive to collisional stabilisation and/or internal reorganisation and dissociation to HNO + CO_2. Petty *et al.*,[19] by observing HOCO directly, determined rate constants for the overall reaction between NO and HOCO at two different total pressures, 3.2–3.5 Torr and 6.6–6.7 Torr, CO_2 being used as the diluent gas. The rate constant at the higher CO_2 pressure was slightly larger but no greater than the combined experimental errors from the two series of experiments. In terms of the mechanism given above, the experiments of Petty *et al.*[19] would yield a rate constant:

$$ k_4 = k_a \left\{ \frac{k_p + k_M[\text{M}]}{k_d + k_p + k_M[\text{M}]} \right\} $$

The rate constants measured in Petty *et al.*'s experiments would only have shown a noticeable pressure-dependence if, under their conditions, k_p and k_M[M] and k_d and $k_p + k_M$[M]

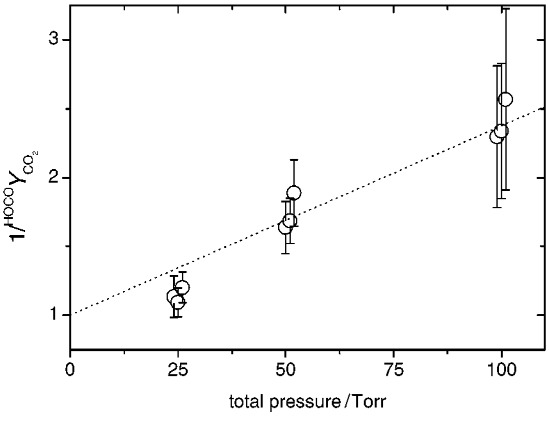

Fig. 6 Reciprocals of the CO_2 yields from the NO + HOCO reaction plotted against total pressure.

Table 3 Rate constant values for the reactions (3)–(7) used in simulations described in the text, the results of which are shown in the Fig. 4

Reaction		Rate constant	Remarks
$HOCO + O_2 \rightarrow HO_2 + CO_2$	(3)	$k_3 = 1.9 \times 10^{-12}$ cm^3 molecule^{-1} s^{-1}	Ref. 19
$HOCO + NO \rightarrow$ products	(4)	$k_4 = 2.45 \times 10^{-12}$ cm^3 molecule^{-1} s^{-1}	Ref. 19
		$^{HOCO}Y_{CO_2} = (k_{4a}/k_4)^a$	This work
$HOCO + NO \rightarrow HNO + CO_2$	(4a)	$k_{4a} = (^{HOCO}Y_{CO_2})k_4$	See text
$HOCO + NO \rightarrow HNO_2 + CO$	(4b)	$k_{4b} = 0.0$	See text
$HOCO + NO + M \rightarrow HOC(O)NO + M$	(4c)	$k_{4c} = (1 - {}^{HOCO}Y_{CO_2})k_4$	See text
$Cl + HCOOH \rightarrow HCl + HOCO$	(5)	k_5[HCOOH] = 810 s^{-1}	This work, from $HOCO + O_2$ studies
$Cl + NO + M \rightarrow ClNO + M$	(6)	$k_3 = 5.1 \times 10^{-32}$ cm^6 molecule^{-2} s^{-1}	This work
$Cl + ClNO \rightarrow Cl_2 + NO$	(7)	$k_3 = 8.1 \times 10^{-11}$ cm^3 molecule^{-1} s^{-1}	Ref. 2

[a] Derived from the analysis in Fig. 6: $\frac{k_{4a}}{k_4} = \frac{k_p}{(k_p + k_{He}[He])} = \frac{1}{(1 + 0.014(p_{He}/Torr)}$.

were of comparable magnitude. Even allowing for differences in the diluent gas between their experiments (CO_2) and ours (He), our results would suggest that k_M[M] would be much less than k_p under the conditions of their experiments. Consequently, no significant pressure effects should have been expected in Petty *et al.*'s experiments. However, the magnitude of the rate constant which they measured, does suggest that k_d is unlikely to be much larger than k_p.

We have performed kinetic simulations of our experimental observations and show an example of these in Fig. 4. In the case of added O_2, only reactions (5) and (3) were included in the model, and, in the case of added NO, reactions (4) to (7) were included. Under our experimental conditions, the rate of formation of CO_2 was largely determined by the rate of reaction (5) between Cl atoms and HCOOH rather than reactions (3) and (4). Consequently, we chose to use the values of k_3 and k_4 found by Petty *et al.*[19] in the simulations, rather than attempt to determine them from our own experiments. Because of some uncertainty associated with the partial pressure of HCOOH introduced into the reaction *via* the bubbler (see above), the pseudo-first-order rate constant, k_5[HCOOH], was derived from the experiments with added O_2 and then used in the experiment with added NO. The values for k_6 and k_7 were those referred to above. The yield of CO_2 from the NO + HOCO reaction was derived from the analysis given in Fig. 6. The rate constants used to simulate the results shown in Fig. 4 are summarised in Table 3. The traces of infrared absorbance in the presence of NO were matched well by the simulations, as shown in Fig. 4, increasing confidence in the interpretation of our results.

We suggest that the difference in behaviour between the reactions of HOCO with NO and O_2 must reflect a difference in the rate at which the energised collision complexes that can be formed in these two systems can undergo internal transfer of an H atom. This process may be faster in the case of $HOCO + O_2$ for two reasons. Firstly, whereas HOC(O)NO is a closed shell molecule, the corresponding species $HOC(O)O_2$ is a free radical. Secondly, the transfer of an H atom in the complex $\{HOC(O)O_2\}^*$ to yield $HO_2 + CO_2$ will proceed *via* a 5-membered cyclic transition state, whilst the formation of $HNO + CO_2$ from $\{HOC(O)NO\}^*$ requires passage through a more strained 4-membered cyclic transition state. For both these reasons, the rate of decomposition of the energised complex is likely to be faster in the case of O_2 + HOCO and make it less likely that collisional stabilisation can compete under the conditions of our experiments.

It is of some interest to compare the results on the reactions of HOCO with O_2 and NO with those of experiments on the reactions of the radicals FCO and CH_3CO, which are iso-electronic with HOCO, with O_2 and NO. Kinetic studies on the reactions of FCO with O_2 and NO at 295 K show that both reactions proceed exclusively by collisionally mediated association.[26] There are, of course, no H atoms in these systems to undergo relatively facile internal transfer. The results of Wallington *et al.*[27] indicate values for the limiting high pressure rate constants of $(1.2 \pm 0.2) \times 10^{-12}$ cm^3 molecule^{-1} s^{-1} for $FCO + O_2$ and $(1.0 \pm 0.2) \times 10^{-12}$ cm^3 molecule^{-1} s^{-1} for FCO + NO. These values are close to those obtained for the overall reactions of HOCO with O_2 and NO and listed in Table 1, suggesting that the overall rates of both these reactions are probably determined by the rates of formation of the energised complexes. Data on the reactions of CH_3CO are less clearcut. In flow tube experiments at total pressures between 1 and 4 Torr, McDade *et al.*[28] determined a pressure-independent rate constant of 9.3×10^{-13} cm^3 molecule^{-1} s^{-1}, which seems likely to correspond to the high pressure rate constant for association. The $CH_3CO + O_2$ reaction has been studied in extensive relative rate measurements by Tyndall *et al.*[29] They found pressure-dependent rate constants and interpreted them in terms of a mechanism like the one that we have used to explain our results. Above 20 Torr, they found the yield of acetyl peroxy radicals to be greater than 90% and the overall reaction to have a limiting high pressure rate constant of $(3.2 \pm 0.6) \times 10^{-12}$ cm^3 molecule^{-1} s^{-1}. The rate constant decreased at pressures below about 20 Torr until between 0.1 and 2 Torr it reached a constant value of $(7 \pm 2) \times 10^{-13}$ cm^3 molecule^{-1} s^{-1}. The results at low pressure were interpreted in terms of decomposition of the energised acetyl peroxy radicals, although the yield of CH_2CO was found to be surprisingly low.

To conclude: we have obtained clear evidence for a new, associative, pathway in the reaction between NO and HOCO which has not been suspected previously. The presumed product is the species HOC(O)NO. Our failure to detect CO as a reaction product indicates that the formation of HONO + CO in the reaction between NO and HOCO is at most a minor channel. We present a discussion that provides a consistent explanation of the reactions of the iso-electronic radicals FCO, HOCO and CH_3CO with O_2 and NO.

Acknowledgements

We are grateful to EPSRC and NERC for research grants and to EPSRC for the award of a studentship (M.C.O). Li Qiang thanks the Royal Society and the Chinese Academy of Sciences for the award of a China Royal Fellowship. We are grateful to Professor C. B. Moore for useful comments on a preliminary draft of this paper.

References

1 R. Atkinson, D. L. Baulch, R. A. Cox, R. F. Hampson, Jr., J. A. Kerr, M. J. Rossi and J. Troe, *J. Phys. Chem. Ref. Data*, 1997, **26**, 521.

2 W. B. DeMore, S. P. Sander, D. M. Golden, R. F. Hampson, Jr., M. J. Kurylo, C. J. Howard, A. R. Ravishankara, C. E. Kolb and M. J. Molina, *Chemical Kinetics and Photochemical Data for Use in Stratospheric Modeling*, JPL Publication, Jet Propulsion Laboratory, Pasadena, CA, 1997, 97-4.

3 J. Brunning, D. W. Derbyshire, I. W. M. Smith and M. D. Williams, *J. Chem. Soc., Faraday Trans. 2*, 1988, **84**, 105.

4 M. J. Frost, P. Sharkey and I. W. M. Smith, *J. Phys. Chem.*, 1993, **89**, 12254.

5 R. Forster, M. Frost, D. Fulle, H. F. Hamann, H. Hippler, A. Schlepegrell and J. Troe, *J. Chem. Phys.*, 1995, **103**, 2949.

6 D. Fulle, H. F. Hamann, H. Hippler and J. Troe, *J. Chem. Phys.*, 1996, **105**, 983; D. Fulle, H. F. Hamann, H. Hippler and J. Troe, *J. Chem. Phys.*, 1996, **105**, 1001.

7 B. Ruscic, M. Schwartz and J. Berkowitz, *J. Chem. Phys.*, 1989, **91**, 6780.

8 M. Alagia, N. Balucani, P. Casavecchia, D. Stranges and G. G. Volpi, *J. Chem. Phys.*, 1993, **98**, 8341.

9 M. J. Frost, P. Sharkey and I. W. M. Smith, *Faraday Discuss. Chem. Soc.*, 1993, **91**, 305.

10 S. Koppe, T. Laurent, P. D. Naik, H.-R. Volpp and J. Wolfrum, *Proc. Int. Symp. Combust.*, 1996, **26**, 489.

11 A. Jacobs, M. Wahl, R. Weller and J. Wolfrum, *Chem. Phys. Lett.*, 1989, **158**, 161.

12 G. Radhakrishan, S. Buelow and C. Wittig, *J. Chem. Phys.*, 1986, **84**, 727.

13 N. F. Scherer, C. Sipes, R. B. Bernstein and A. H. Zewail, *J. Chem. Phys.*, 1990, **92**, 1990.

14 S. I. Ionov, H. F. Davis, K. Mikhaylichenko and L. Valachovic, R. A. Beaudet and C. Wittig, *J. Chem. Phys.*, 1994, **101**, 4809.

15 D. E. Milligan and M. E. Jacox, *J. Chem. Phys.*, 1971, **54**, 927.

16 M. E. Jacox, *J. Chem. Phys.*, 1988, **88**, 4598.

17 T. J. Sears, W. M. Fawzy and P. M. Johnson, *J. Chem. Phys.*, 1992, **97**, 3996.

18 (*a*) J. T. Petty and C. B. Moore, *J. Chem. Phys.*, 1993, **99**, 47; (*b*) J. T. Petty and C. B. Moore, *J. Mol. Spectrosc.*, 1993, **161**, 149.

19 J. T. Petty, J. A. Harrison and C. B. Moore, *J. Phys. Chem.*, 1993, **97**, 11194.

20 J. Nolte, J. Grussdorf, F. Temps and H. Gg. Wagner, *Z. Naturforsch. A*, 1993, **48**, 1234.

21 A. Miyoshi, H. Matsui and N. Washida, *J. Chem. Phys.*, 1994, **100**, 3532.

22 M. C. Osborne, Qiang Li and I. W. M. Smith, *Phys. Chem. Chem. Phys.*, 1999, **1**, 1447.

23 M. C. Osborne, Qiang Li and I. W. M. Smith, *Int. J. Chem. Kinet.*, 2000, **32**, 85.

24 T. J. Wallington, J. M. Andino, J. C. Ball and S. M. Japar, *J. Atmos. Chem.*, 1990, **10**, 301.

25 M. J. Howard and I. W. M. Smith, *Prog. Reac. Kinet.*, 1983, **12**, 55.

26 Y. Ninomiya, M. Goto, S. Hashimoto, M. Kawasaki and T. J. Wallington, *Int. J. Chem. Kinet.*, 2001, **33**, 130.

27 T. J. Wallington, T. Ellermann, O. J. Nielsen and J. Sehested, *J. Phys. Chem.*, 1994, **98**, 2346.

28 C. M. McCade, T. M. Lenhardt and K. D. Bayes, *J. Photochem.*, 1982, **20**, 1.

29 G. S. Tyndall, J. J. Orlando, T. J. Wallington and M. D. Hurley, *Int. J. Chem. Kinet.*, 1997, **29**, 655.